nks

A Procedure to Generate Input Data of Cyclic Softening and Hardening for FEM Analysis from Constant Strain Amplitude Fatigue Tests in LCF Regime

Urpo Sarajärvi and Otso Cronvall
VTT, Finland

March 2007

Abstract

Fatigue is produced by cyclic application of stresses by mechanical or thermal loading. The metal subjected to fluctuating stress will fail at stresses much lower than those required to cause fracture in a single application of load. The key parameters are the range of stress variation and the number of its occurrences. Low-cycle fatigue, usually induced by mechanical and thermal loads, is distinguished from high-cycle fatigue, mainly associated with vibration or high number of small thermal fluctuations.

Numerical models describing fatigue behaviour of austenitic stainless piping steels under cyclic loading and their applicability for modelling of low-cycle-fatigue are discussed in this report.

In order to describe the cyclic behaviour of the material for analysis with finite element method (FEM) based analysis code ABAQUS, the test data, i.e. stress-strain curves, have to be processed. A code to process the data all through the test duration was developed within this study. A description of this code is given also in this report. Input data for ABAQUS was obtained to describe both kinematic and isotropic hardening properties. Further, by combining the result data for various strain amplitudes a mathematic expression was be created which allows defining a parameter surface for cyclic (i.e. isotropic) hardening. Input data for any strain amplitude within the range of minimum and maximum strain amplitudes of the test data can be assessed with the help of the developed 3D stress-strain surface presentation.

The modelling of the fatigue induced initiation and growth of cracks was not considered in this study. On the other hand, a considerable part of the fatigue life of nuclear power plant (NPP) piping components is spent in the phase preceding the initiation and growth of cracks.

Key words

A Procedure to Generate Input Data of Cyclic Softening and Hardening for FEM Analysis from Constant Strain Amplitude Fatigue Tests in LCF Regime

Authors   Sarajärvi, Urpo, Cronvall, Otso

Confidentiality   Public

Report's title		
A Procedure to Generate Input Data of Cyclic Softening and Hardening for FEM Analysis from Constant Strain Amplitude Fatigue Tests in LCF Regime		
Customer, contact person, address STUK		Order reference
Project name INPUT VÄSYMA		Project number/Short name 3573/
Author(s) Sarajärvi, Urpo, Cronvall, Otso		Pages 31/
Keywords Fatigue, low-cycle, austenitic stainless steel, work hardening, modelling, FEM, ABAQUS		Report identification code VTT-R-11555-06

Summary

Fatigue is produced by cyclic application of stresses by mechanical or thermal loading. The metal subjected to fluctuating stress will fail at stresses much lower than those required to cause fracture in a single application of load. The key parameters are the range of stress variation and the number of its occurrences /1/.

Low-cycle fatigue, usually induced by mechanical and thermal loads, is distinguished from high-cycle fatigue, mainly associated with vibration or high number of small thermal fluctuations /1/.

Numerical models describing fatigue behaviour of austenitic stainless piping steels under cyclic loading and their applicability for modelling of low-cycle-fatigue are discussed in this report.

In order to describe the cyclic behaviour of the material for analysis with finite element method (FEM) based analysis code ABAQUS, the test data, i.e. stress-strain curves, have to be processed. A code to process the data all through the test duration was developed within this study. A description of this code is given also in this report. Input data for ABAQUS was obtained to describe both kinematic and isotropic hardening properties. Further, by combining the result data for various strain amplitudes a mathematic expression was be created which allows defining a parameter surface for cyclic (i.e. isotropic) hardening. Input data for any strain amplitude within the range of minimum and maximum strain amplitudes of the test data can be assessed with the help of the developed 3D stress-strain surface presentation.

The modelling of the fatigue induced initiation and growth of cracks was not considered in this study. On the other hand, a considerable part of the fatigue life of nuclear power plant (NPP) piping components is spent in the phase preceding the initiation and growth of cracks.

Confidentiality	Public

Espoo 14.2.2007
Signatures

Eila Lehmus   Urpo Sarajärvi
Technology Manager   Research Scientist

VTT's contact address
P.O. Box 1000, FI-02044 VTT

Distribution (customer and VTT)

STUK: Registry (4), Keskinen R. (1), Hytönen Y. (1); FNS: Neuvonen A. (1);
TVO: Pulkkinen E. (1 kpl); NKS (1); VTT: Archive (1)

Preface

This report has been prepared under the research project INPUT VÄSYMA. The project is a part of SAFIR, which is a national nuclear energy research program. In the structure of SAFIR, this research project is a subproject of project INPUT, which is a part of a larger project system INTELI. INPUT stands for Reactor circuit piping, and INTELI stands for Integrity and lifetime of reactor circuits. The work was carried out at VTT. VÄSYMA project was funded by the State Nuclear Waste Management Fund (VYR), Nordic nuclear safety research (NKS; NKS-R Framework) and the Technical Research Centre of Finland (VTT).

Espoo

Authors

Contents

List of symbols

Latin symbols

C_{ijkl}	constitutive tensor (rank 4)
E	elastic modulus
f	yield function
F	total deformation gradient matrix
$\mathbf{F}^{el}$	matrix of fully recoverable part of the deformation
$\mathbf{F}^{pl}$	matrix of non-recoverable part of the deformation
g	plastic potential
H	plastic modulus
k	current yield stress in shear
t	time
u	vector of displacements
U	strain energy density potential
T	temperature
x	vector of current location of the material point
X	vector of initial location of the material particle

Greek symbols

β	back stress tensor
ε	strain matrix
$\dot{\varepsilon}$	matrix of total (mechanical) strain rate
ε^{pl}	matrix of plastic strain
$\dot{\varepsilon}^{el}$	matrix of elastic strain rate
$\dot{\varepsilon}^{pl}$	matrix of plastic strain rate
ε_{ij}	strain tensor (rank 2)
κ	hardening variable
λ, μ	Lamé coefficients
ρ	back stress tensor
σ	stress matrix
σ^0	size of the yield surface
σ_{ij}	stress tensor (rank 2)
σ_y	yield stress
σ_u	stress at rupture
σ^*	matrix of initial stresses
ξ	internal variables

List of abbreviations

BWR	boiling water reactor
CSSC	cyclic stress train curve
FEA	finite element analysis
FEM	finite element method
LWR	light water reactor
NPP	nuclear power plant
ORNL	Oak Ridge National Laboratory
PWR	pressurised water reactor
RPV	reactor pressure vessel
VTT	Technical Research Centre of Finland

1 Introduction

Fatigue is produced by cyclic application of stresses by mechanical or thermal loading. The metal subjected to fluctuating stress will fail at stresses much lower than those required to cause fracture in a single application of load. The key parameters are the range of stress variation and the number of its occurrences. Technological conditions (i.e. surface roughness and residual stresses) and environmental conditions (presence of deleterious chemical species) may also play a role /1/.

Low-cycle fatigue, usually induced by mechanical and thermal loads, is distinguished from high-cycle fatigue, mainly associated with vibration or high number of small thermal fluctuations /1/.

One characteristic of fatigue in metals is work hardening under reversed loading conditions. With continued cyclic loading, the rate of hardening progressively diminishes and a quasi-steady state of deformation, known as saturation, is reached. Once saturation occurs, the variation of the resolved shear stress with the resolved shear strain is not altered by further load cycles and the stress-strain hysteresis loop develops a stable configuration. Naturally work hardening behaviour is a material specific phenomenon /2/. Eventually, after a material, stress amplitude and temperature dependent number of load cycles, component fails, which e.g. typically occurs so that macroscopic cracks first initiate, and then grow and coalesce, which finally leads to rupture.

Numerical models describing fatigue behaviour of austenitic stainless piping steels under cyclic loading and their applicability for modelling of low-cycle-fatigue are discussed in this report.

In order to describe the cyclic behaviour of the material for analysis with finite element method (FEM) based analysis code ABAQUS, the test data, i.e. stress-strain curves, have to be processed. A code to process the data all through the test duration was developed within this study, see also references /20, 21/. A description of this code is given also in this report. With the code it is possible e.g. to assess the elastic and work hardening ranges for each load cycle in the test data. The code was used for processing of data from constant strain amplitude fatigue tests performed to specimens of austenitic stainless steel.

The modelling of the fatigue induced initiation and growth of cracks was not considered in this study. On the other hand, a considerable part of the fatigue life of nuclear power plant (NPP) piping components is spent in the phase preceding the initiation and growth of cracks.

The structure of this report is the following. An overview of fatigue degradation in nuclear power plant (NPP) piping systems is presented first. This is followed with a review of models for metals subjected to cyclic loading. This includes discussion of e.g. yield surfaces and yield criteria, hardening rules and ORNL constitutive model. The report then moves on to describe how the behaviour of metals subjected to cyclic loading can be modelled with ABAQUS. The hardening and softening characteristics of the analysed constant strain amplitude fatigue test data are discussed next. This issue as well as the next one concerning parameter surfaces for the elastic range includes a presentation of the application of the fatigue test data processing analysis tool developed within the project. The report ends with conclusions.

2 Goal

The goals of this study are to numerically simulate the behaviour of metals subjected to cyclic loading with FEM code ABAQUS, to analyse constant strain amplitude fatigue test data, and to develop a fatigue test data processing analysis tool. All these goals were achieved during the four years duration of this study, see references /20, 21, 22/. The goal was to develop such an analysis tool with which one can e.g. both calculate cyclically certain relevant characteristic values, e.g. elastic range, and form a set of certain cyclical parameter values needed as a part of ABAQUS analysis input files. Another goal in the development of the analysis tool was to include a capability to trim the analysed data, and consequently resulting hardening parameters. The need for the trimming arose from the fact that the analysed fatigue test data presents some scatter caused by the limited accuracy of the test equipment and the sampling rate. The hardening parameters to be obtained from the application analysis results are to be used in the subsequent ABAQUS analyses, and then the fatigue test data can be compared with the ABAQUS simulation results.

3   Fatigue in the nuclear power plant piping systems and characteristics of low-cycle fatigue

Fatigue is the primary degradation mechanism associated with NPP piping. A distinction can be made between components subject to low cycle fatigue (approximately 10 000 cycles or less) and those subject to high cycle fatigue (greater than 10 000 cycles). Generally, low cycle fatigue conditions are characterised by high amplitude load (stress, strain or strain rate) and shorter lifetimes /1/.

The main fatigue mechanism affecting pressurised water reactor (PWR) primary coolant piping is low-cycle fatigue caused by a combination pressure and transient thermal stresses. The points of stress concentration in the system are the areas of most concern. These locations include terminal ends of the piping. In boiling water reactor (BWR) plants degradation due to fatigue is more severe to the reactor pressure vessel (RPV) than to piping systems /3/.

Fatigue damage in a pipe first occurs at a micro-structural level before manifesting itself as a macroscopic crack, and a further period of crack growth may occur before failure. Certain factors can increase the likelihood of defect initiation and/or growth rate. These can include environmentally assisted mechanisms, such as corrosion and localised high concentrations of chlorides, shape imperfections in a welded joint, such as misalignment and undercut, the application of post weld heat treatment and the combination of the amplitude and frequency of the applied stresses /4/.

In thermal fatigue of a piping component alternating stresses caused by thermal cycling results in accumulated fatigue usage and can lead to crack initiation and growth. Austenitic and carbon steel piping segments with operating temperatures less than 130 ^{o}C and 100 ^{o}C, respectively, are not susceptible to degradation by thermal fatigue. In the case of thermal transients, areas considered susceptible to thermal fatigue include pipe segments where there is relatively rapid cold water injection with temperature change greater than 95 ^{o}C for austenitic steel pipes and 65 ^{o}C for carbon steel pipes. In the case of thermal stratification and striping, areas where there can be leakage past valves separating hot and cold fluids and regions where there might be intermittent mixing of hot and cold fluids caused by fluid injection, are considered to be susceptible to thermal fatigue induced degradation, except for pipe segments where the pipe diameter is 2.5 cm or less, or the slope of the segment is 45 ^{o} or more from the horizontal /5/.

Vibration fatigue failures are normally a result of poor component design or fabrication practice. The nature of this mechanism is such that, generally, almost the entire fatigue life of the component is expended during the initiation phase. Piping components susceptible to vibration fatigue include e.g. socket welded piping in the immediate vicinity of vibration sources such as pumps /5/.

A more comprehensive description of the fatigue type examined in this report, namely low-cycle fatigue, is presented in the following. An important distinction between low-cycle fatigue and high-cycle fatigue is that in high-cycle fatigue most of the fatigue life is spent in crack initiation, whereas in low-cycle fatigue most of the life is spent in crack propagation, because cracks are found to initiate within 3 to 10 % of the fatigue life. Traditionally in low-

cycle fatigue tests the strain range is held constant and the stresses are allowed to vary. The variation of stresses with strains in low-cycle fatigue typically leads to a hysteresis loop that consists of linear and nonlinear parts. Usually strain is presented in the horizontal axis in these diagrams. The total width of the loop corresponds to total strain range, which can be broken up into the elastic strain range and the plastic strain range. The total height of the hysteresis loop is the stress range. In the course of low-cycle fatigue tests the stress range does not remain constant. With increasing number of load cycles the stress range initially increases or decreases, and eventually reaches an approximately steady value. This is known as the saturation or cyclically stable condition /6/. Eventually, after a material, stress amplitude and temperature dependent number of load cycles, component fails, which e.g. typically occurs so that macroscopic cracks first initiate, and then grow and coalesce, which finally leads to rupture.

4 Models for metals subjected to cyclic loading

4.1 Introduction

A variety of constitutive models is available to describe the material behaviour of metals. For example, a component made from a standard structural steel can be modelled as an isotropic, linear elastic and rate-independent material with no temperature dependence, if loading and other conditions stay within reasonable limits. However, if the component experiences a severe overload, the material could be modelled as rate-independent elastic, perfectly plastic. Or, if the ultimate stress in a tension test of a specimen of the material is very much above the initial yield stress, isotropic work hardening might be included in the plasticity model. A nonlinear analysis, with or without consideration of geometric nonlinearity, should then be performed to the structural model. If the severe overload is applied suddenly, it can cause rapid straining of the material. In such circumstances the inelastic response of metals usually exhibits rate dependence: the flow stress increases as the strain rate increases. A viscoplastic (rate-dependent) material model could then be required. If the concern is not gross overload, but gradual failure of the component because of low cycle fatigue or because of creep at high temperature, or a combination of these effects, then the response of the material during several cycles of loading, in each of which a small amount of inelastic deformation might occur, must be predicted: a circumstance in which the material response needs to be modelled in much more detail.

The constitutive model for a linear elastic material can be defined, using indicial notation, as /7/:

$$\sigma_{ij} = C_{ijkl}\varepsilon_{kl} \tag{4.1}$$

where σ_{ij} is stress tensor (rank 2), C_{ijkl} is constitutive tensor (rank 4) and ε_{ij} is strain tensor (rank 2). The components of the constitutive tensor are dependent of temperature, so they are constants only under isothermal conditions. Expression (4.1) is also called generalised Hooke's law. In the general case the number of components in the constitutive tensor is 81. Under service state loading conditions steel is often modelled as an isotropic linear elastic material. Under isothermal conditions the constitutive tensor of isotropic linear elastic materials is only dependent of Lamé coefficients λ and μ.

When considering plastic properties of steels, the definition of constitutive tensor changes, as its components are dependent of strains in the nonlinear region of the stress-strain curve. Generally speaking the behaviour of steels is dependent of strains, stresses, temperature, strain rate and load history (stress and strain histories). The dependence to strain rate and load history can be represented with so called internal variables. Examples of internal variables are plastic strains and inelastic work /7/.

In addition to nonlinear stress-train relation, sometimes nonlinear strain measures have to be applied. The distinction between different strain measures matters only when the strains are not negligible compared to unity; that is, in finite strain problems. The elastic strains always remain small for many materials of practical interest; for example, the yield stress of a metal is typically three orders of magnitude smaller than its elastic modulus, implying elastic strains

of order 10^{-3} /8/. Examples of commonly applied nonlinear measures for finite strains are Green-Lagrange strain tensor and Cauchy-Green strain tensor /7/.

From a numerical viewpoint the implementation of a constitutive model involves the integration of the state of the material at an integration point over a time increment during a nonlinear analysis /8/.

4.2 Yield surfaces and yield criteria

Rate-independent plastic materials have an elastic range within which they respond in a purely elastic manner. The boundary of this range, in either stress or strain space, is called the yield surface. The shape of the yield surface depends on the entire history of deformation from the reference state. During plastic deformation the states of stress or strain remain on the subsequent yield surfaces. The yield surfaces for actual materials are experimentally found to be mainly smooth, although they may develop pyramidal or conical vertices, or regions of high curvature. If elasticity within the yield surface is linear and unaffected by plastic flow, the yield surfaces for metals are convex in the Cauchy stress space /9/.

Let T denote temperature and ξ denote an array of internal variables ξ_1, ξ_2, ..., ξ_n. If there is a continuous function $f(\sigma, T, \xi)$ such that there exists a region in the space of the stress components in which (at given values of T, ξ) /7/:

$$f(\sigma, T, \xi) < 0 \tag{4.2}$$

and such that the plastic strain rate tensor $\dot{\varepsilon}^{pl}$ vanishes in that region but not outside it, then this region constitutes the elastic range, and $f(\sigma, T, \xi) = 0$ defines the yield surface in stress space. The orientation of the yield surface is defined in such a way that the elastic range forms its interior.

The yield surface can change its size and shape in the stress space. When the yield surface expands it is said that material hardens and when it contracts it is said that material softens. The dependence of the yield function f on the internal variables ξ describes what are usually called hardening properties of the material /7/.

Stress states that cause the yield function to have a positive value cannot occur in rate-independent plasticity models, although this is possible in a rate-dependent model /8/.

It has been observed that the effect of hydrostatic pressure, which corresponds to mean stresses in the stress matrix, to the yielding of steels (and most metals) is negligible. Instead, the yielding of steels is dependent of shear deformations, and hence of shear stresses. However, for metals under conditions of high triaxial tension when voids may nucleate and grow in the material, the dependence of mean stresses can be of significance. Such conditions can arise in stress fields near crack tips and in some extreme thermal loading cases such as those which might occur during welding processes /8/.

Some of the most commonly used yield criteria for metallic materials are:
- Tresca yield criterion; it embodies the assumption that plastic deformation occurs when the maximum shear stress over all planes attains the value of the current yield stress in shear, its projection in the principal stress-deviator plane is a hexagon /7/.

- Von Mises yield criterion; also known as the maximum octahedral shear-stress criterion, its projection in the principal stress-deviator plane is an ellipse /7/.
- Hill yield criterion; is a simple extension of the Mises yield function to allow for anisotropic behaviour, it can be expressed in terms of rectangular Cartesian stress components /11/.

Besides yield surface and yield criteria, two other concepts are needed as well in order to be able to describe the plastic behaviour of metallic materials. These are the flow rule and the hardening rule. The former rule is briefly described in the following, whereas rules concerning the latter concept are due to their importance described in more detail in the next Section.

According to flow rule the plastic strains in yield surface expansion/contraction must be directed along the outward normal of it. This flow rule definition is also known as the normality rule. An associated flow rule is such that the plastic potential related to it is the yield condition, whereas a nonassociated flow rule is such that the plastic potential related it is distinct from the yield condition.

4.3 Hardening rules

A specification of the dependence of the yield criterion on the internal variables, along with the rate equations for these variables, is called a hardening rule.

Isotropic hardening

Many yield functions are reducible to the form:

$$f(\boldsymbol{\sigma}, \xi) = F(\boldsymbol{\sigma}) - k(\xi) \tag{4.3}$$

Since it is only the yield stress that is affected by the internal variables, no generality is lost if it is assumed to depend on only one internal variable, say ξ_1, and this is invariably identified with the hardening variable κ, defined as either the plastic work or as the effective plastic strain.

Isotropic hardening can be modelled with yield functions having the form presented in (4.3). Isotropic hardening represents a global expansion of the yield surface, with no change in shape. Thus for a given yield criterion and flow rule, hardening behaviour in any process can be predicted from the knowledge of the function $k(\xi)$, and this function may, in principle, be determined from a single test (such as a tension test). The usefulness of the isotropic hardening model in approximating real behaviour is limited. In uniaxial stressing it predicts that when a certain yield stress σ_y has been attained as a result of work hardening, the yield stress encountered on stress reversal is just $-\sigma_y$, a result clearly at odds with the Bauschinger effect. Furthermore, if $F(\boldsymbol{\sigma})$ is an isotropic function, then the yield criterion remains isotropic even after plastic deformation has taken place, so that the model cannot describe induced anisotropy.

Kinematic hardening

When yield function f can be written in the form:

$$f(\boldsymbol{\sigma}, \xi) = F(\boldsymbol{\sigma} - \boldsymbol{\rho}) - k(\xi) \tag{4.4}$$

then more general hardening behaviour can be described. Isotropic hardening is a special case of (4.4) if $\boldsymbol{\rho} \equiv 0$ and if k depends only on κ, while purely kinematic hardening corresponds to constant k but nonvanishing variable $\boldsymbol{\rho}$, which is a tensor in stress space, sometimes called the back stress. Kinematic hardening represents a translation of the yield surface in stress space by shifting its reference point from the origin to $\boldsymbol{\rho}$, and with uniaxial stressing this means that the length of the stress interval representing the elastic region (i.e., the difference between the current yield stress and the one found on reversal) remains constant. This is in fairly good agreement with the Bauschinger effect for those materials whose stress-strain curve in the work-hardening range can be approximated by a straight line ("linear hardening"), and it is for such materials that Melan /12/ proposed the model in which $\boldsymbol{\rho} = c\boldsymbol{\varepsilon}^{pl}$, with c a constant. A generalisation of this idea was performed by Prager /13,14/. A kinematic hardening model is also capable of representing induced anisotropy, since a function $F(\boldsymbol{\sigma} - \boldsymbol{\rho})$ that depends only on the invariants of its argument stops being an isotropic function of the stress tensor as soon as $\boldsymbol{\rho}$ differs from zero.

In more sophisticated kinematic hardening models, internal variables other than $\boldsymbol{\varepsilon}^{pl}$ and κ are included; in particular, the back stress $\boldsymbol{\rho}$ may be treated as a tensorial internal variable with its own rate equation.

Generalised hardening rules

A model with a family of back stresses $\boldsymbol{\rho}_{(l)}$ ($l = 1, 2, ..., n$) was developed by Mróz /15/; a similar model was developed by Iwan /16/. Both models describe materials whose stress-strain curves are piecewise linear. For materials whose stress-strain curves in the work-hardening range are smooth with straight-line asymptotes, a class of models known as two-surface models have been proposed by Dafalias /17/, Krieg /18/, and others. In these models the yield surface in stress space is constrained to move inside an outer surface, known variously as bounding surface, loading surface, or memory surface, given by, say:

$$\bar{f}(\boldsymbol{\sigma}, \xi) = 0 \tag{4.5}$$

The various two-surface models differ from one another in the definition of the bounding surface, in the way the image stress depends on the current state and in the variation of plastic modulus H. In the model of Dafalias and Popov /19/, both surfaces are given similar combined hardening structures, with a "back stress" $\boldsymbol{\beta}$ playing the same role for the outer surface that $\boldsymbol{\rho}$ plays for the yield surface, and $\bar{\boldsymbol{\sigma}} = c(\boldsymbol{\sigma} - \boldsymbol{\rho}) + \boldsymbol{\beta}$, where c is a constant.

4.4 Cyclic hardening with plastic shakedown

Cyclic hardening with plastic shakedown is characteristic of symmetric stress or strain controlled experiments. Soft or annealed metals tend to harden toward a stable limit, and initially hardened metals tend to soften. Figure 4.1 illustrates the behaviour of a metal that hardens under prescribed symmetric strain cycles /8/.
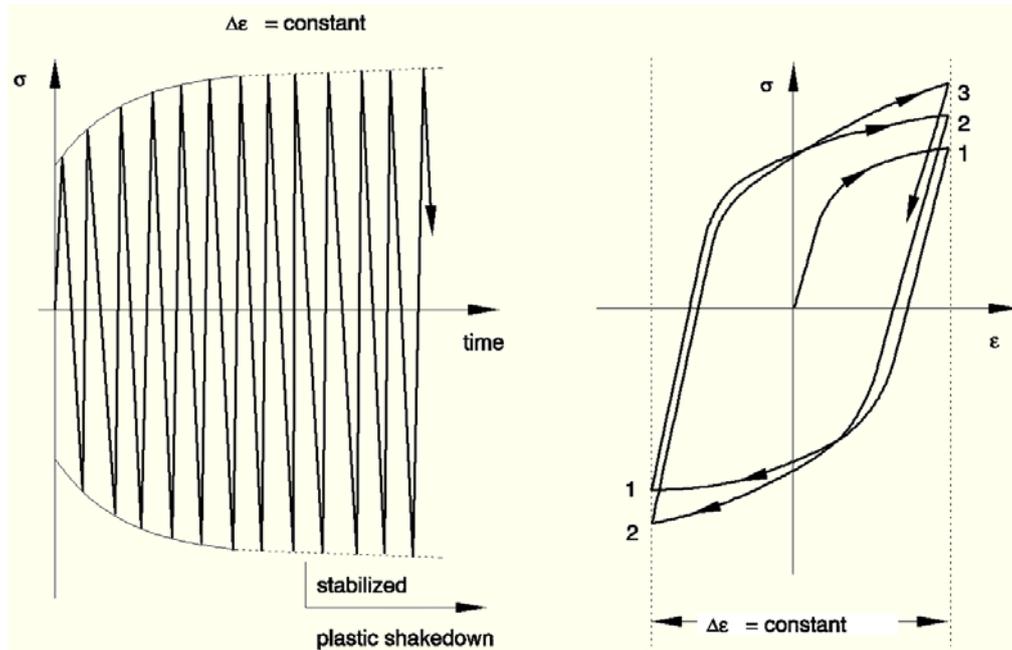
Figure 4.1. Plastic shakedown /8/.

4.5 ORNL constitutive model

The Oak Ridge National Laboratory (ORNL) constitutive model is intended for cyclic loading and high-temperature creep of type 304 and 316 stainless steel. Plasticity and creep calculations are provided according to the specification in Nuclear Standard NEF 9-5T, "Guidelines and Procedures for Design of Class I Elevated Temperature Nuclear System Components." This model is an extension of the linear kinematic hardening model, which attempts to provide for simple life estimation for design purposes when low-cycle fatigue and creep fatigue are critical issues.

The ORNL constitutive model adds isotropic hardening of the plastic yield surface from a virgin material state to a fully cycled state. Initially the material is assumed to harden kinematically according to a bilinear representation of the virgin stress-strain curve. If a strain reversal takes place or if the creep strain reaches 0.2 %, the yield surface expands isotropically to the user-defined tenth cycle stress-strain curve. Further hardening occurs kinematically according to a bilinear representation of the tenth-cycle stress-strain curve.

The ORNL constitutive model assumes that the work hardening formulation is used with creep.

In the following is a brief description of the theory of the ORNL model. The ORNL constitutive theory is uncoupled into a rate-independent plasticity response and a rate-dependent creep response, each of which is governed by a separate constitutive law. The plasticity theory uses a Von Mises yield surface that can expand isotropically and translate kinematically in stress space. Nuclear standard NE F9-5T provides for some coupling between the plasticity and creep responses by allowing prior creep strain to expand and translate the subsequent yield surface in stress space. For Types 304 and 316 stainless steel, however, prior plasticity does not change the subsequent creep response.

A set of auxiliary creep and load reversal detection rules, using modified work hardening creep theory, overcomes the inconsistencies usually encountered with standard work

hardening theories under a stress reversal. In particular, creep theories based on work hardening assumptions predict creep rates that are too small under conditions of stress reversal, so that the amount of creep that occurs under cyclic loading conditions will generally be underestimated.

The plasticity theory for stainless steels, as set forth in nuclear standard NE F9-5T, employs a Von Mises yield surface with kinematic hardening. Normally, when combined isotropic and kinematic hardening is considered, the centre of the yield surface is assumed to translate linearly with plastic strain according to a Prager or Ziegler kinematic hardening rule. Incorporation of isotropic hardening into the constitutive formulation then changes the form of the stress-strain relation but leaves the Prager or Ziegler kinematic shift rule for determining the motion of the centre of the yield surface intact. In the ORNL plasticity formulation the form of the stress-strain law is left intact (a bilinear representation in one dimension), and modifications to the kinematic shift rule are made to accommodate isotropic hardening.

The expansion of the yield surface is approximated by a step change in the value of σ^0, which is the size of the yield surface Figure 4.2 shows the value of σ^0 appropriate to the initial stress-strain curve, $\sigma^0_0(\theta)$, and the value of σ^0 appropriate to the 10th cycle curve, $\sigma^0_{10}(\theta)$.
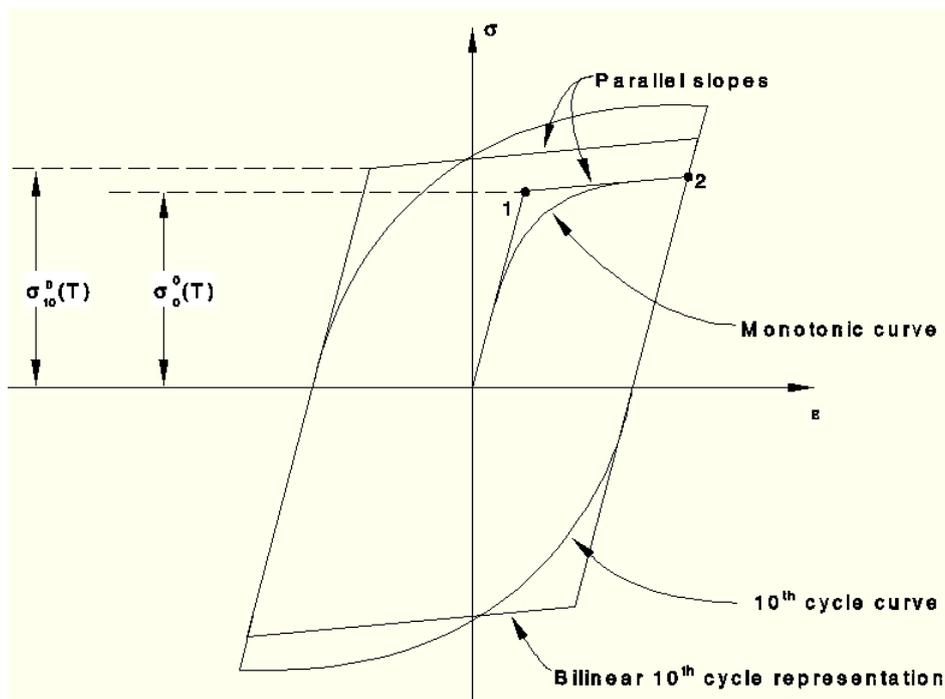

Figure 4.2. The initial and 10th cycle ORNL stress-strain curves are assumed to have equal slopes in the plastic portion of the bilinear representation /8/.

A step change in the size of the yield surface occurs when yielding first occurs after stress reversal. Nuclear standard NE F9-5T recommends that the yield surface centre remain fixed during the step change in σ^0. The plastic tangent modulus of the 10th cycle stress-strain curve is the same as the plastic tangent modulus of the initial stress-strain curve. This requirement is also necessary so that the 10th cycle stress-strain curve under fully reversed strain controlled loading is symmetric about the stress-strain origin.

5 Modelling of the behaviour of metals subjected to cyclic loading with ABAQUS

5.1 Introduction

The kinematic hardening models in ABAQUS are intended to simulate the behaviour of metals that are subjected to cyclic loading. These models are typically applied to studies of low-cycle fatigue and ratchetting. The basic concept of these models is that the yield surface shifts in stress space so that straining in one direction reduces the yield stress in the opposite direction, thus simulating the Bauschinger effect and anisotropy induced by work hardening.

Two kinematic hardening models are available in ABAQUS. The simplest model provides linear kinematic hardening and is, thus, mainly used for low-cycle fatigue evaluations. This model yields physically reasonable results if the uniaxial behaviour is linearised in the plastic range (a constant work hardening slope). This is usually best accomplished by guessing the strain levels that will be attained in the problem and linearising the actual material behaviour accordingly. It is important to recognise this restriction on the ability of the theory to provide reasonable results and to provide material data accordingly. This model is available with the Von Mises or Hill yield surface.

The combined isotropic/kinematic hardening model is an extension of the linear model. It provides a more accurate approximation to the stress-strain relation than the linear model. It also models other phenomena, such as ratchetting, relaxation of the mean stress and cyclic hardening, which are typical of materials subjected to cyclic loading. This model is available only with the Von Mises yield surface.

Only strain rate independent behaviour of metals is considered in this study. The notation of equations used in this chapter is that used in the ABAQUS documentation /8/.

5.2 Elastic and plastic behaviour

The elastic behaviour can be modelled with ABAQUS only as linear elastic:

$$\boldsymbol{\sigma} = \mathrm{D}^{el} : \boldsymbol{\varepsilon} \tag{5.1}$$

where D^{el} represents the fourth order elasticity tensor and $\boldsymbol{\sigma}$ and $\boldsymbol{\varepsilon}$ are the second order stress and strain tensors, respectively. This equation is the same as equation (4.1) presented in Chapter 4.

The available models for plastic behaviour are pressure independent plasticity models. For these models the yield surface is defined by the function:

$$f(\boldsymbol{\sigma} - \boldsymbol{\alpha}) = \sigma^0 \tag{5.2}$$

where $f(\boldsymbol{\sigma} - \boldsymbol{\alpha})$ is the equivalent Von Mises stress or Hill's potential with respect to the back stress or "kinematic shift" $\boldsymbol{\alpha}$, and σ^0 is the size of the yield surface. The equivalent Von Mises stress is defined as:

$$f(\boldsymbol{\sigma} - \boldsymbol{\alpha}) = \sqrt{\frac{3}{2}\left(S - \boldsymbol{\alpha}^{dev}\right):\left(S - \boldsymbol{\alpha}^{dev}\right)} \tag{5.3}$$

where $\boldsymbol{\alpha}^{dev}$ is the deviatoric part of the back stress and S is the deviatoric stress tensor.

These models assume associated plastic flow as:

$$\dot{\boldsymbol{\varepsilon}}^{pl} = \frac{\partial f(\boldsymbol{\sigma} - \boldsymbol{\alpha})}{\partial \boldsymbol{\sigma}} \dot{\bar{\varepsilon}}^{pl} \tag{5.4}$$

where $\dot{\boldsymbol{\varepsilon}}^{pl}$ represents the rate of plastic flow and $\dot{\bar{\boldsymbol{\varepsilon}}}^{pl}$ is the equivalent plastic strain rate, which is defined as:

$$\dot{\bar{\boldsymbol{\varepsilon}}}^{pl} = \sqrt{\frac{2}{3}\dot{\varepsilon}^{pl}:\dot{\varepsilon}^{pl}} \tag{5.5}$$

5.3   Linear kinematic hardening model

This model is the simpler of the two kinematic hardening models available in ABAQUS. The size of the yield surface, $\sigma^0(\theta)$, can be a function of temperature only for this model. The evolution of $\boldsymbol{\alpha}$ is defined by Ziegler's hardening rule, generalised to the nonisothermal case as:

$$\dot{\boldsymbol{\alpha}} = C\dot{\bar{\boldsymbol{\varepsilon}}}^{pl}\frac{1}{\sigma^0}(\boldsymbol{\sigma} - \boldsymbol{\alpha}) + \frac{1}{C}\boldsymbol{\alpha}\dot{C} \tag{5.6}$$

where $C(\theta)$ is the hardening parameter ($C(\theta)$ is the work-hardening slope of the isothermal uniaxial stress-strain response, $d\boldsymbol{\sigma}/d\bar{\boldsymbol{\varepsilon}}^{pl}$, taken at different temperatures) and $\dot{C}$ is the rate of change of C with respect to temperature. This form of evolution law for $\boldsymbol{\alpha}$ defines the rate of $\boldsymbol{\alpha}$ due to plastic straining to be in the direction of the current radius vector from the centre of the yield surface, $\boldsymbol{\sigma} - \boldsymbol{\alpha}$, and the rate due to temperature changes to be toward the origin of stress space. Rice (1975) writes this concept quite generally as:

$$\dot{\boldsymbol{\alpha}} = \dot{\mu}(\boldsymbol{\sigma} - \boldsymbol{\alpha}) + h\boldsymbol{\alpha}\dot{\theta} \tag{5.7}$$

The particular identification of $\dot{\mu} = C\dot{\bar{\boldsymbol{\varepsilon}}}^{pl}/\sigma^0$ and $h = (dC/d\theta)/C$ in Equation 5.7 above is assumed, so the material behaviour is defined by the isothermal, uniaxial work hardening data, $C(\theta)$ only.

5.4 Nonlinear isotropic/kinematic hardening model

This model is based on the work of Lemaitre and Chaboche /23/. The size of the yield surface, $\sigma^0\left(\bar{\varepsilon}^{pl},\theta,f_i\right)$, is defined as a function of equivalent plastic strain $\bar{\varepsilon}^{pl}$, temperature θ and field variables f_i. This dependency can be provided directly, can be coded in user subroutine UHARD, or can be modelled with a simple exponential law for materials that either cyclically harden or soften as:

$$\sigma^0 = \sigma\big|_0 + Q_\infty\left[1 - \exp\left(-b\bar{\varepsilon}^{pl}\right)\right] \tag{5.8}$$

where $\sigma\big|_0(\theta,f_i)$ is the yield surface size at zero plastic strain, and $Q_\infty(\theta,f_i)$ and $b(\theta,f_i)$ are additional material parameters that must be calibrated from cyclic test data.

The evolution of the kinematic component of the model is defined as:

$$\dot{\boldsymbol{\alpha}} = C\dot{\bar{\boldsymbol{\varepsilon}}}^{pl}\frac{1}{\sigma^0}(\boldsymbol{\sigma}-\boldsymbol{\alpha}) - \gamma\boldsymbol{\alpha}\dot{\bar{\boldsymbol{\varepsilon}}}^{pl} + \frac{1}{C}\boldsymbol{\alpha}\dot{C}$$

where C and γ are material parameters, with $\dot{C}$ representing the rate of change of C with respect to temperature and field variables. The rate of change of γ with respect to temperature and field variables is not accounted for in the model. This equation is the basic Ziegler law, generalised to account for temperature and field variable dependency of C, and to which a "recall" term $\gamma\boldsymbol{\alpha}\dot{\bar{\boldsymbol{\varepsilon}}}^{pl}$ has been added. The recall term introduces the nonlinearity in the evolution law.

5.5 Limitations of the hardening models

The linear kinematic model is a simple model that gives only a first approximation of the behaviour of metals subjected to cyclic loading. The nonlinear isotropic/kinematic hardening model can provide more accurate results in many cases involving cyclic loading, but it still has the following limitations:

- The isotropic hardening is the same at all strain ranges. Physical observations, however, indicate that the amount of isotropic hardening depends on the magnitude of the strain range. Furthermore, if the specimen is cycled at two different strain ranges, one followed by the other, the deformation in the first cycle affects the isotropic hardening in the second cycle. Thus, the model is only a coarse approximation of actual cyclic behaviour. It should be calibrated to the expected size of the strain cycles of importance in the application.
- The same cyclic hardening behaviour is predicted for proportional and nonproportional load cycles. Physical observations indicate that the cyclic hardening behaviour of materials subjected to nonproportional loading may be very different from uniaxial behaviour at similar strain amplitude.

6 Hardening and softening during fatigue test

6.1 Behaviour of the stress amplitude

As mentioned earlier, in commonly applied and generally accepted plasticity theory the basic concept with which material hardening and softening can be approached is the yield surface. The shape of the yield surface depends on the entire history of deformation from the reference state.

As mentioned earlier, the yield surface can change its size and shape in the stress space. The hardening and softening can be illustrated by looking at a case of uniaxial stress in two specimens of metal alloy analysed in this study, the stress amplitude curves of which are shown as a function of experienced load cycles in Fig. 6.1. Besides the steeply descending short end parts, during ascending curve parts the specimens harden and during descending parts they soften, i.e. during the former parts the yield limit rises, and during the latter parts it lowers. As mentioned earlier, both of these curves have abruptly descending, almost vertical end parts, during which macroscopic cracks first initiate, and then grow and coalesce, which finally leads to rupture of the specimens.
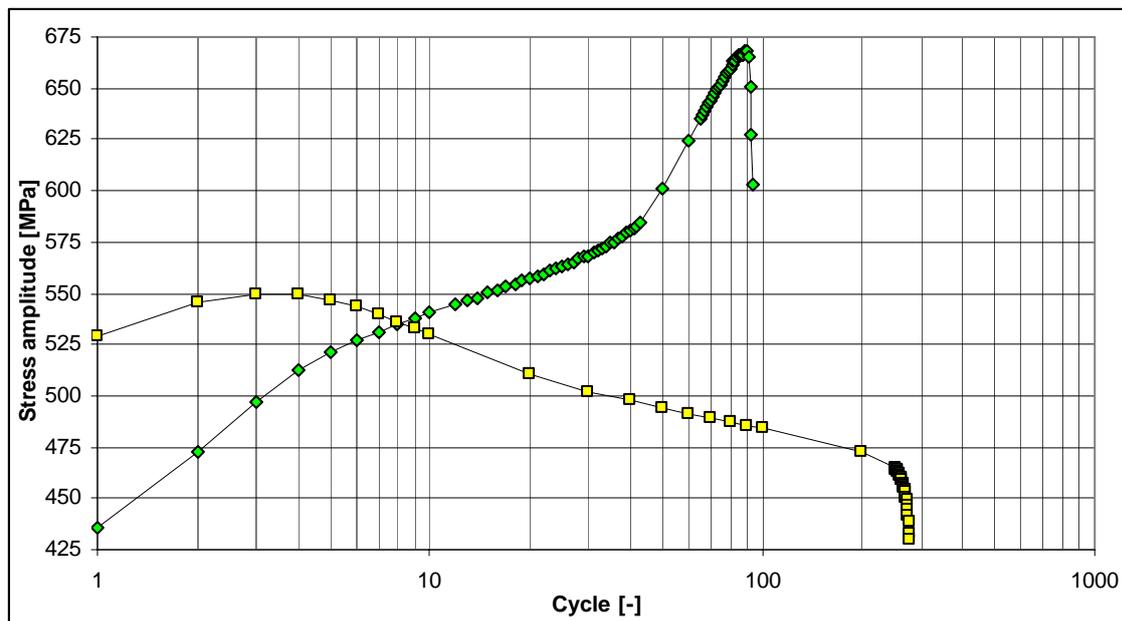
Figure 6.1. Samples of hardening and softening. Besides the steeply descending short end parts, during ascending curve parts the specimens harden, and during descending parts they soften.

Another and more detailed example of cyclic metal hardening and softening is presented in Fig. 6.2. In the enlarged detail figures of the various stages of hardening and softening the limits of accuracy of the test equipment start to show too, as most of the points forming the curve in question deviate slightly from the smooth curve path.
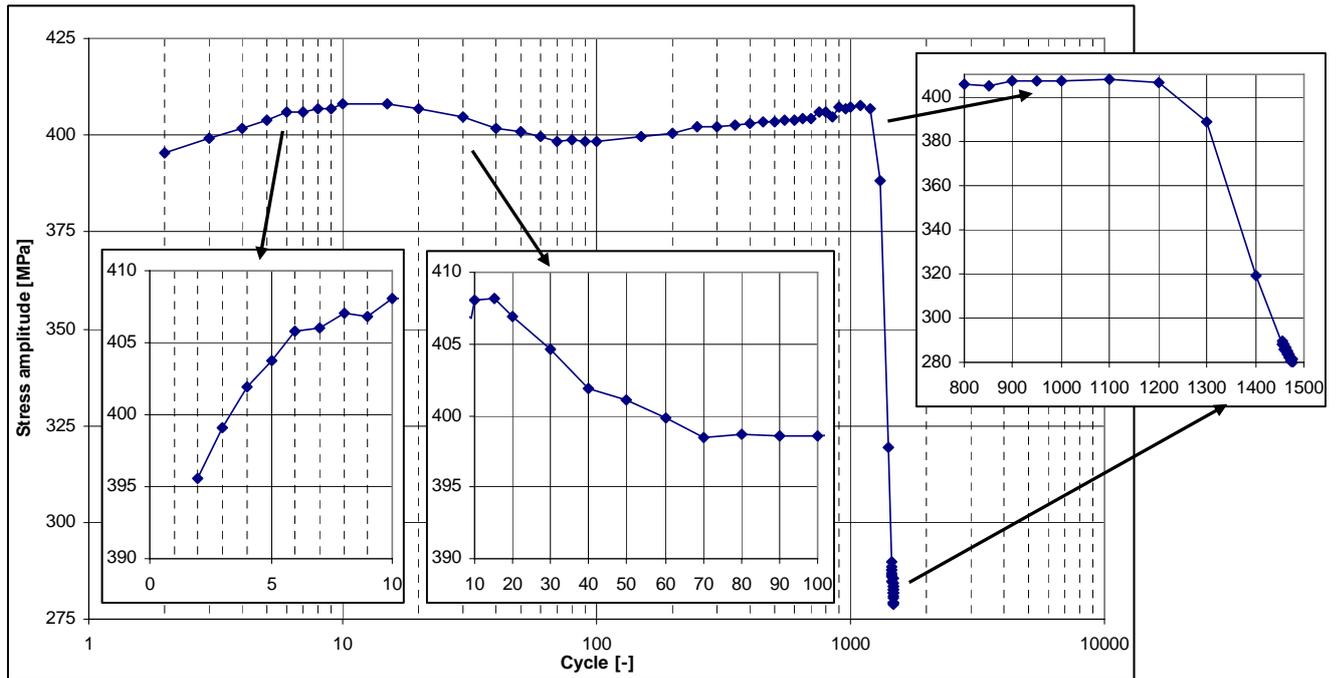
Figure 6.2   Stages of hardening and softening.

The dependence of the yield function on the internal variables describes usually the hardening/softening properties of the material /7/.

For the metal alloy analysed in this study there are examples in the following Figs. 6.3 to 6.5 showing: cyclic hardening during the first load cycles, gradual softening during the consequent load cycles, and final hardening and breaking down.
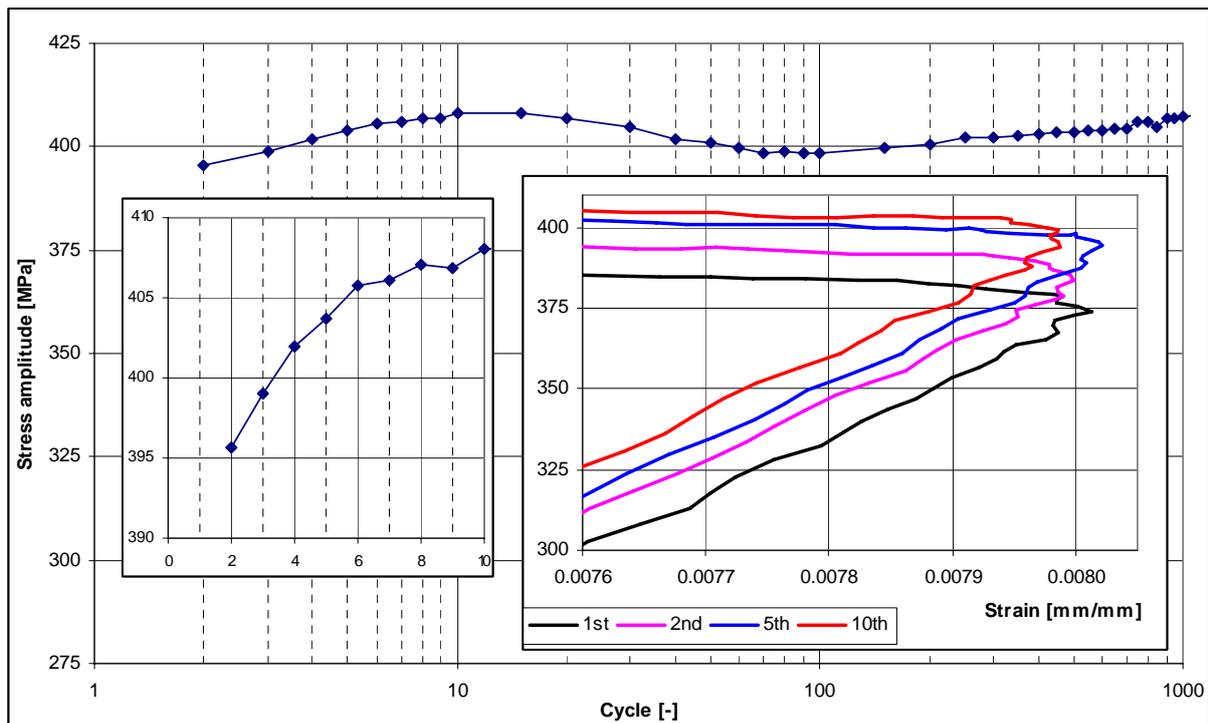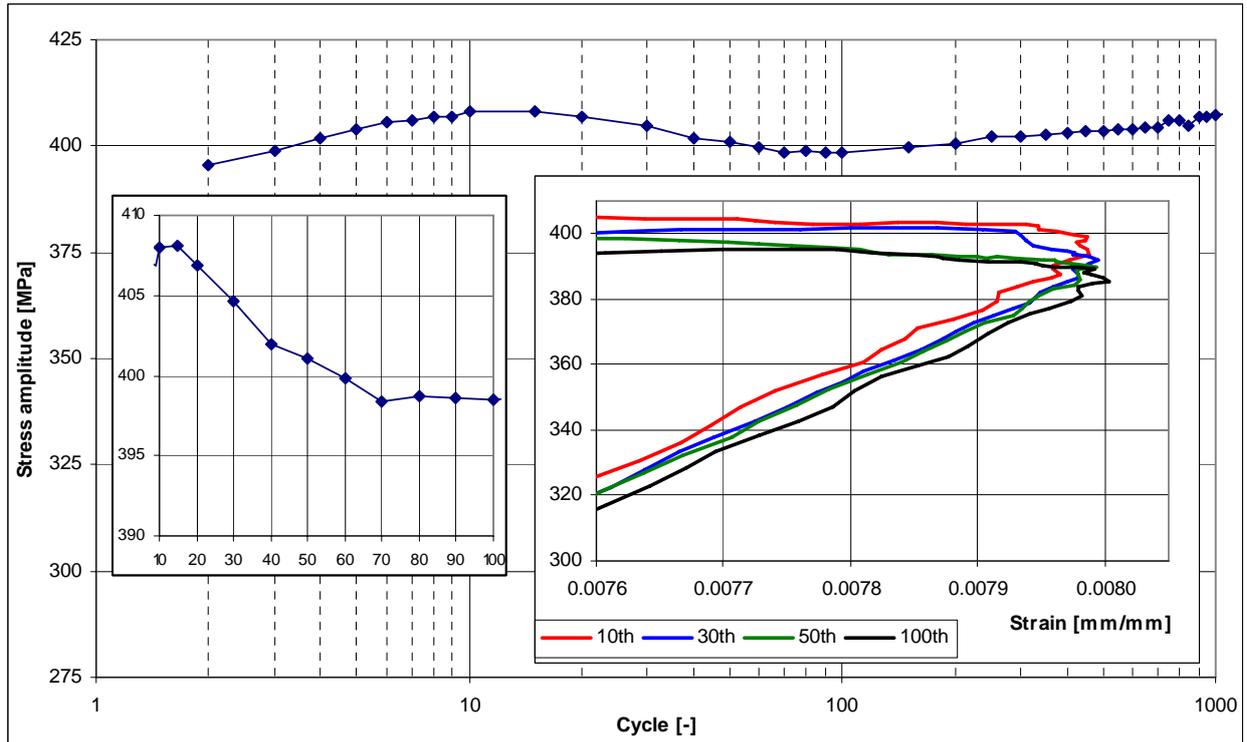

Figure 6.3.   Hardening during the first load cycles.

Figure 6.4.   Gradual softening after the first load cycles.
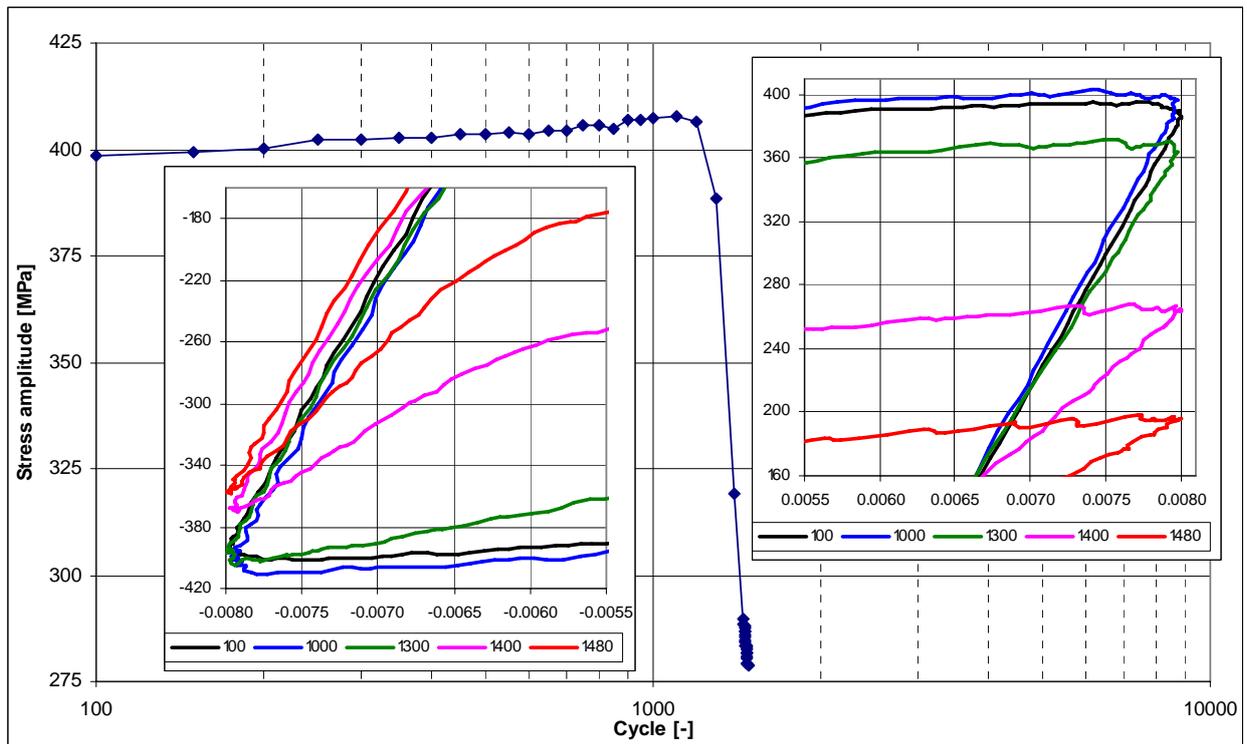
Figure 6.5   Final hardening and breaking down.

6.2 Definition of hardening parameters

6.2.1 Processing of the fatigue test data

In order to describe the behaviour of the material for ABAQUS analysis the test data, i.e. stress-strain curves, have to be processed. A code to process the data all through the test duration is reported in references /20, 21/. Below (Fig. 6.6) there is a short illustration of the procedure.

For each cycle the yield stress in compression is determined as the point where stress curve crosses a straight line corresponding to the selected plastic strain (strain offset parallel to slope of the curve start). The elastic range is the difference between the peak stress and the yield stress. Correspondingly the yield stress in tension is the valley stress with the addition of the elastic range. The elastic range varies as a function of softening and hardening of the material. The code mentioned above defines these two elastic ranges for each load cycle in the test data. Sample results are described in Ch. 6.2.3.
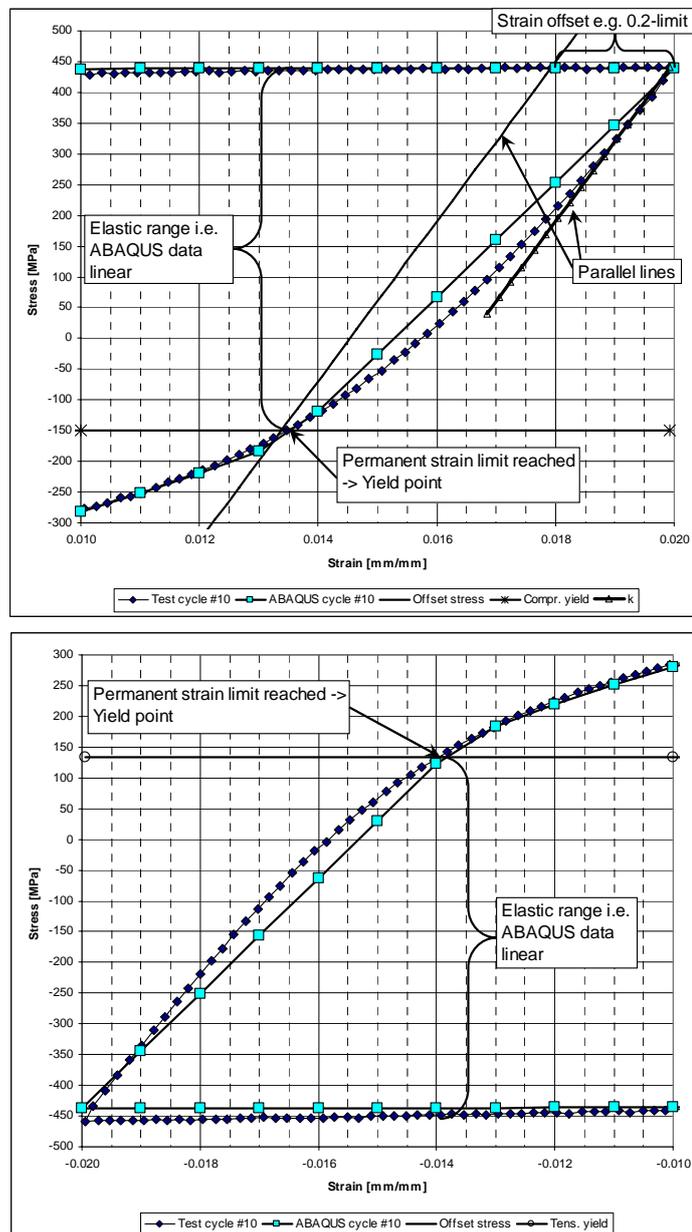

Figure 6.6   Graphical illustration of elastic range definition /20/.

6.2.2 Kinematic hardening

One of the parameters needed in the ABAQUS fatigue analyses is that concerning kinematic hardening. It describes the form of the stress-strain curve in the plastic zone. The tenth cycle is assumed to represent a stabilized cycle and is selected to describe the kinematic hardening. In reference /20/ there are a couple of results reported, but here all of the test data is considered. Fig. 6.7 shows the kinematic hardening of all the test data for the analysed austenitic base material. Tests were done with five different strain amplitudes, two of which comprising two or three tests. Lower strain amplitude tends to produce lower hardening, though the start point, i.e. yield stress, appears to vary so that the curves cross each other.

The effect of using different forms of kinematic hardening is studied in reference /21/. The best compatibility with test data is reached by using the kinematic hardening of the test with the same strain amplitude as in the FEM analysis. Though, the difference between test data and results from FEM analysis remains well below 10% if the kinematic hardening of the highest strain amplitude is used (Fig. 6.8).
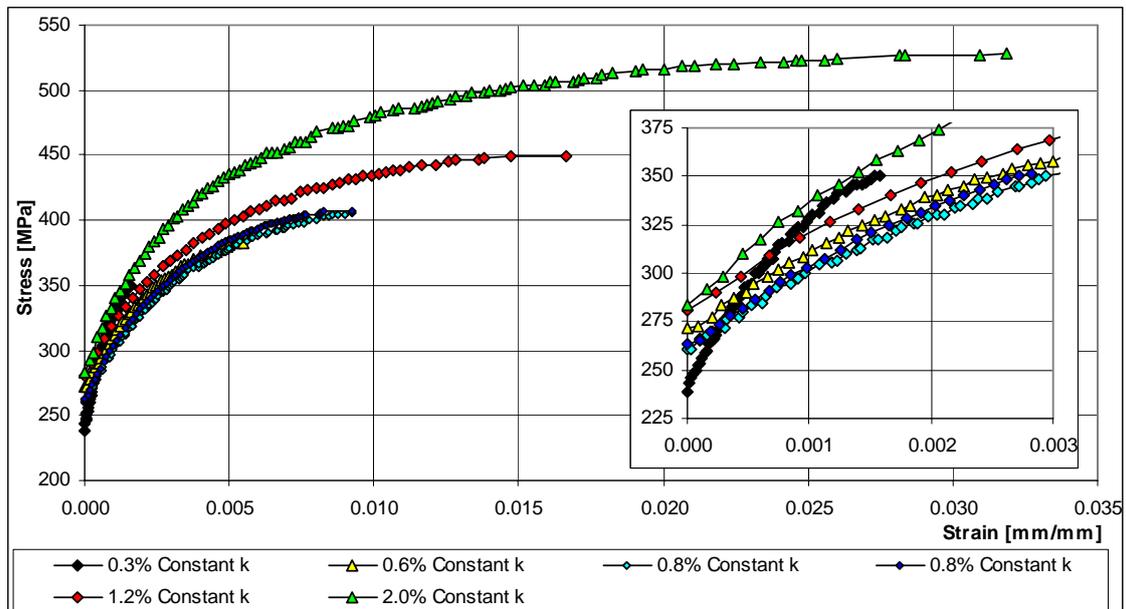

Figure 6.7   Kinematic hardening of austenitic base material with various strain amplitudes.
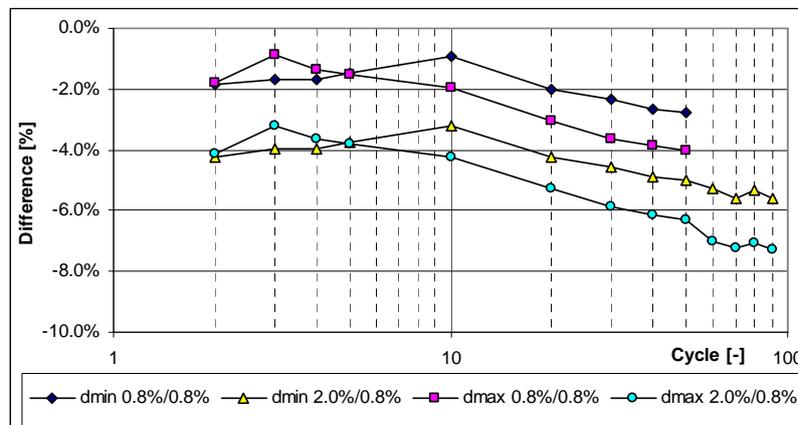

Figure 6.8   Comparison between differences in minimum and maximum stresses (0.8%/0.8%= both kinematic and cyclic hardening by strain amplitude of 0.8%, 2.0%/0.8%= kinematic hardening by strain amplitude of 2.0% and cyclic hardening by strain amplitude of 0.8%)

6.2.3 Cyclic hardening

Another parameter needed in the ABAQUS fatigue analyses is that concerning cyclic hardening. It defines the progress of the elastic range when loading is repeated. The cyclic hardening is described as the elastic range in stress units (MPa in SI units) per equivalent plastic strain in strain units (mm/mm). In reference /20/ a couple of cases are introduced and all test data is gathered together in reference /21/. Fig. 6.9 illustrates the cyclic hardening of the analysed austenitic base material. As previously in Chap. 6.2.2, tests were done with five different strain amplitudes, two of which comprising two or three tests. The material has a hardening tendency, especially with high strain amplitudes.
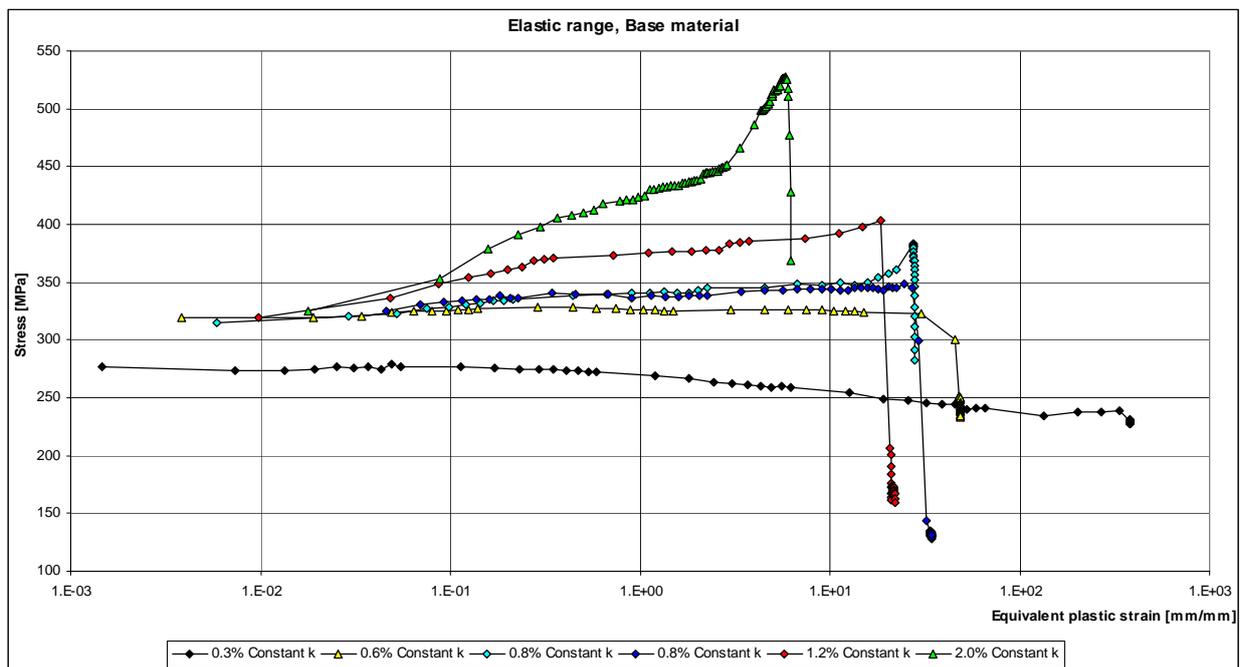

Figure 6.9   Elastic ranges of austenitic base material with various strain amplitudes.

Different approaches to define the cyclic hardening are described in reference /21/. Bearing in mind that ABAQUS uses only one value for elastic modulus and one shape for the plastic part of the stress-strain curve (kinematic hardening), elastic range is the parameter that varies in the course of softening and hardening. *I.e.* the curves in Fig. 6.9 follow the shape of the curves illustrating the stress amplitude. The final procedure to define elastic range is to:
   - define elastic modulus from the start of the first cycle
   - analyse the first ten cycles in detail to define an average ratio between stress amplitude and elastic range
   - calculate the elastic range for the rest of the cycles by dividing the stress amplitude of each cycle with the ratio

7 Parameter surface for elastic range

In this chapter the elastic ranges for different strain amplitudes are studied more in detail. A set of results was chosen which allows performing an exemplary study. The results shown below do not represent reliable values for a certified FEM analysis, but act as a sample case to describe an approach to develop input data for FEA. In Fig. 7.1 the stress-strain curves are depicted on linear scale cut at equivalent plastic strain 50 mm/mm. Elastic range can be illustrated also at different equivalent plastic strains when strain amplitude is described on abscissa, as in Fig. 7.2. The values for equivalent strain are chosen arbitrarily. The elastic ranges at these equivalent strains were interpolated from the curves in Fig. 7.1.
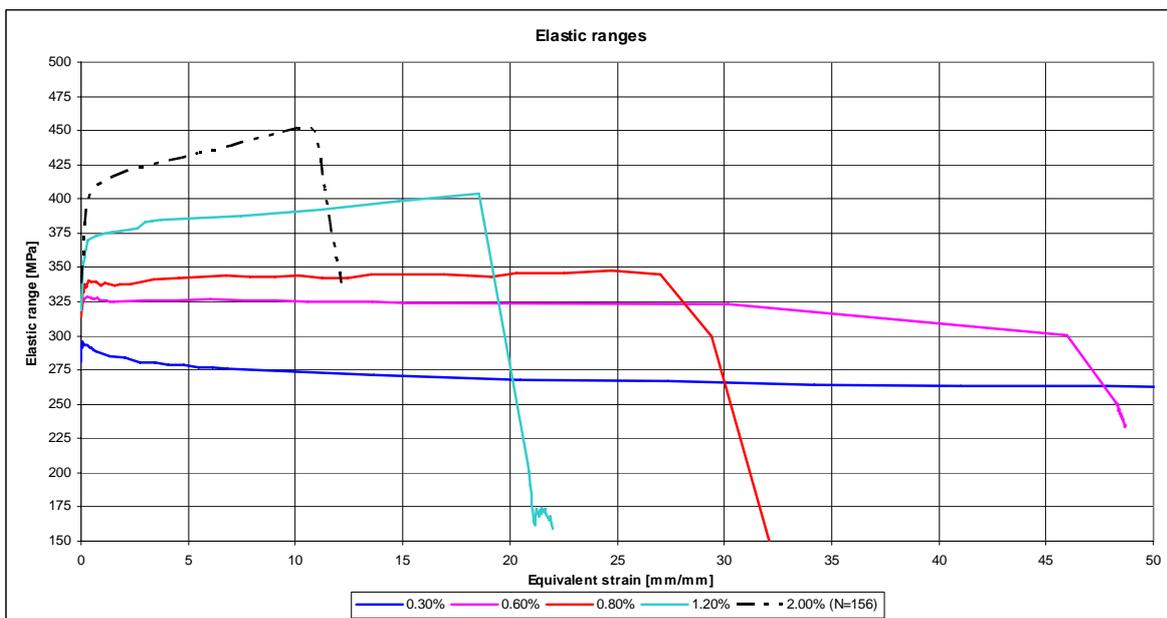

Figure 7.1   Curves for elastic range up to equivalent strain 50 mm/mm (linear scale).
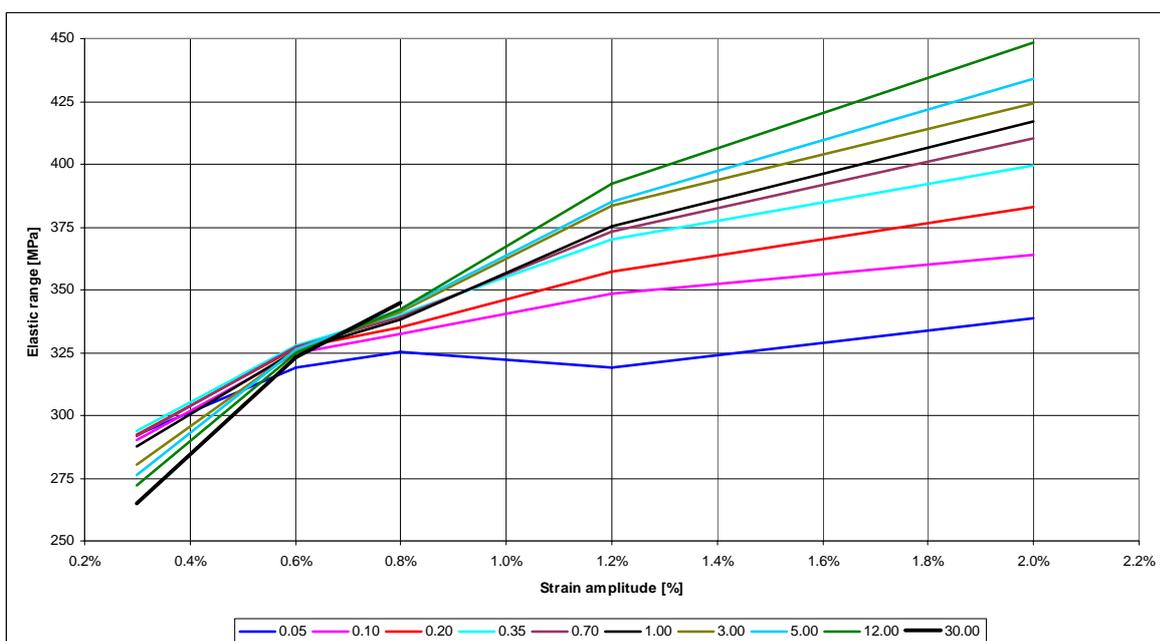

Figure 7.2   Elastic ranges vs. strain amplitude at various plastic equivalent strains.

The stress-strain curves shown in Figs. 7.1 and 7.2 can be joined to a 3D representation either as curves or as a surface (Fig. 7.3). In order to form a mathematical function to describe the surface, the representation for CSSC (cyclic stress-strain curve) in NUREG/CR-5704 was chosen as a starting point. It describes the stress amplitude for various strain amplitudes in the form /24/:

$$\varepsilon_a = (\sigma_a / 1950) + (\sigma_a / A)^B \tag{7.1}$$

where ε_a = strain amplitude [mm/mm], σ_a = stress amplitude [MPa], A and B = material specific parameters.

As mentioned in Ch. 6.2.3, elastic range follows stress amplitude and similar formula can be chosen:

$$\varepsilon_a = (\sigma_a / 290000) + (\sigma_a / A)^B \tag{7.2}$$

where ε_a = strain amplitude [mm/mm]
constant (290000) = 2 * elastic modulus [MPa]
σ_a = elastic range [MPa]
material specific parameters $\left\{ \dfrac{A}{B} \right\} = a + b \cdot \varepsilon_{eq}{}^c \tag{7.3}$

where ε_{eq} = equivalent strain amplitude [mm/mm]
a, b, c = fit parameters

Equation (7.2) defines the elastic range at a certain value of equivalent plastic strain, i.e. one curve in Fig. 7.2. A study was made, to see if the progress of constants A and B could be described with a mathematic formula, resulting to Equation (7.3). In Fig. 7.4 there are data points solved with data shown in Fig. 7.2 and curves fit to the data points according to Equation (7.3). Fit parameters a, b and c are gathered in Table 7.1.

Table 7.1   Fit parameters in Eq. (7.3) solved for sample data.

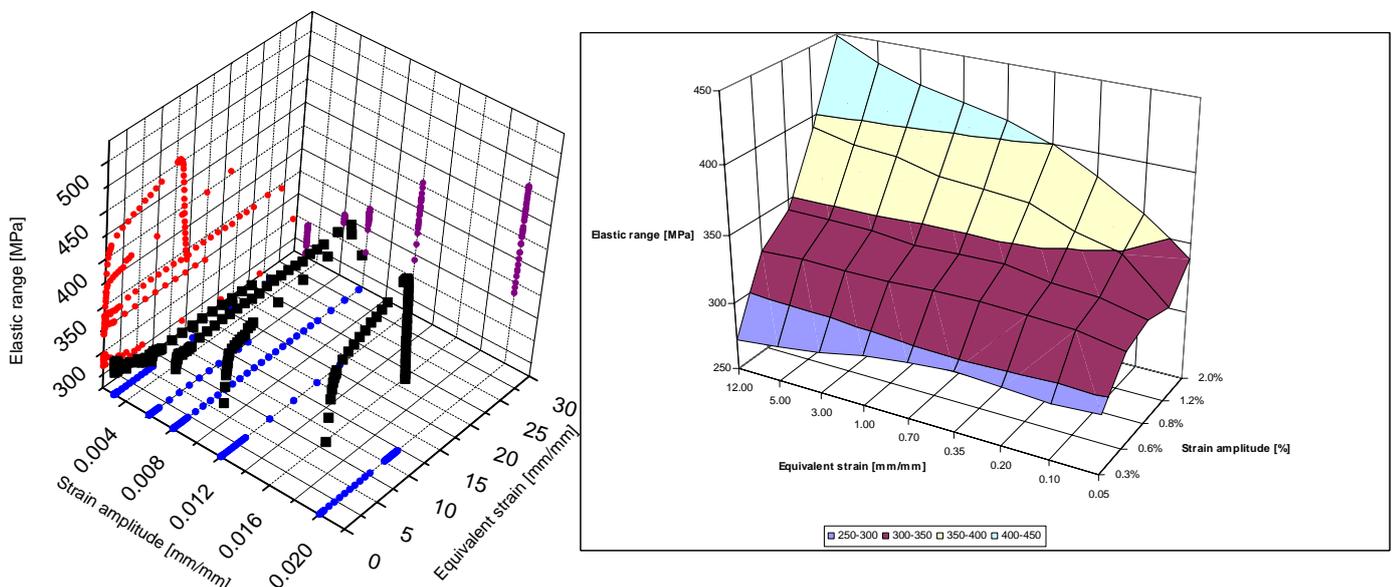|	A	B
a	-2601.676	3.7
b	3420	2
c	0.0415	-0.665

Figure 7.3   Elastic ranges as 3D-curves (left) and a surface (right; arbitrary scales).

Finally, Figure 7.5 illustrates curves for elastic ranges at various equivalent plastic strains. Fig. 7.6 shows the calculated curves as a surface and Fig. 7.7 shows the difference in percents between test data and calculated values. Test data tends to have lower values at low equivalent strains and higher values at higher equivalent strains. Though, this study is more as exemplar. With a more profound statistic analysis more accurate values for the fit parameters and material specific parameters can be determined.
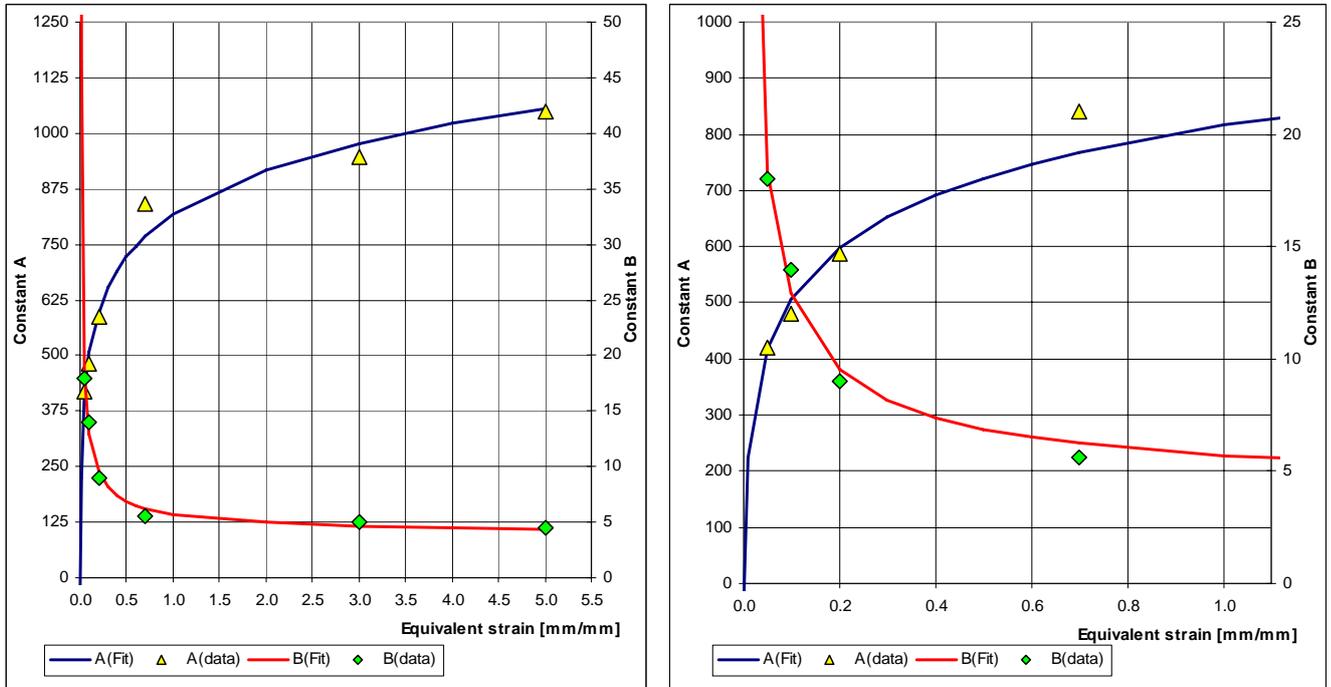

Figure 7.4   Constants A and B at various equivalent strains.
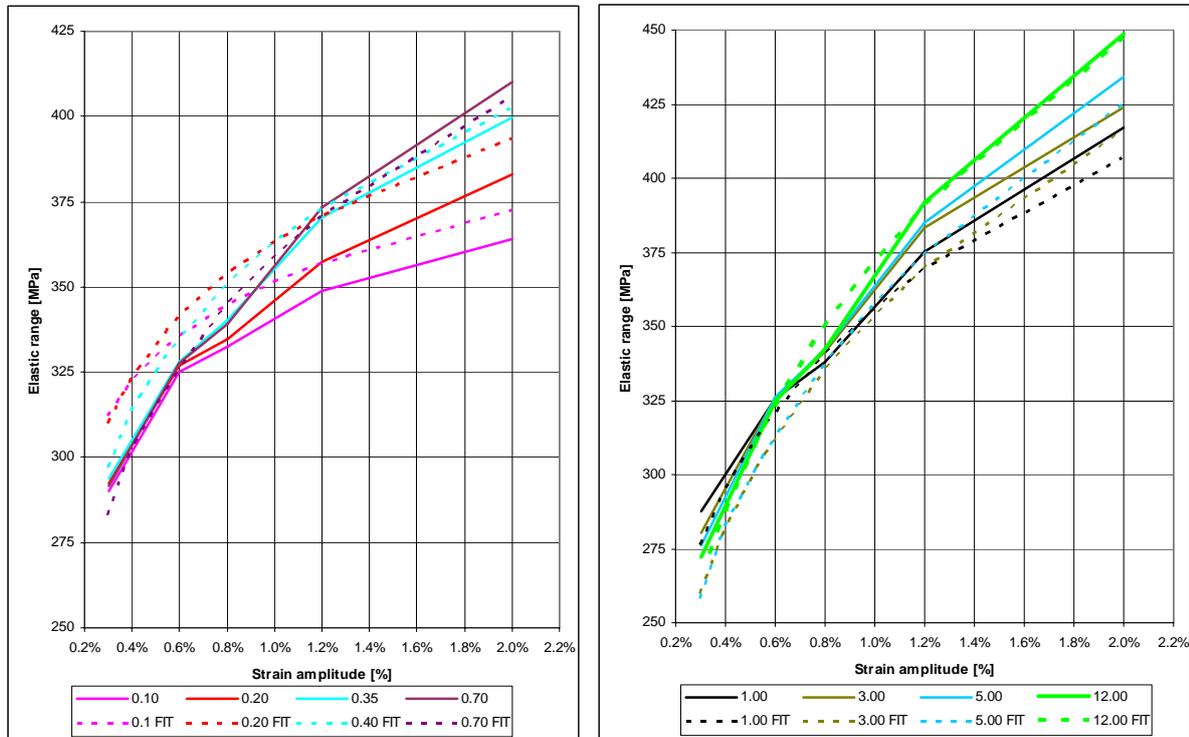

Figure 7.5   Elastic ranges processed from test data and fit curves according to Eq. (7.2).
Left: equivalent strains from 0.1 to 0.7, Right: equivalent strains from 1.0 to
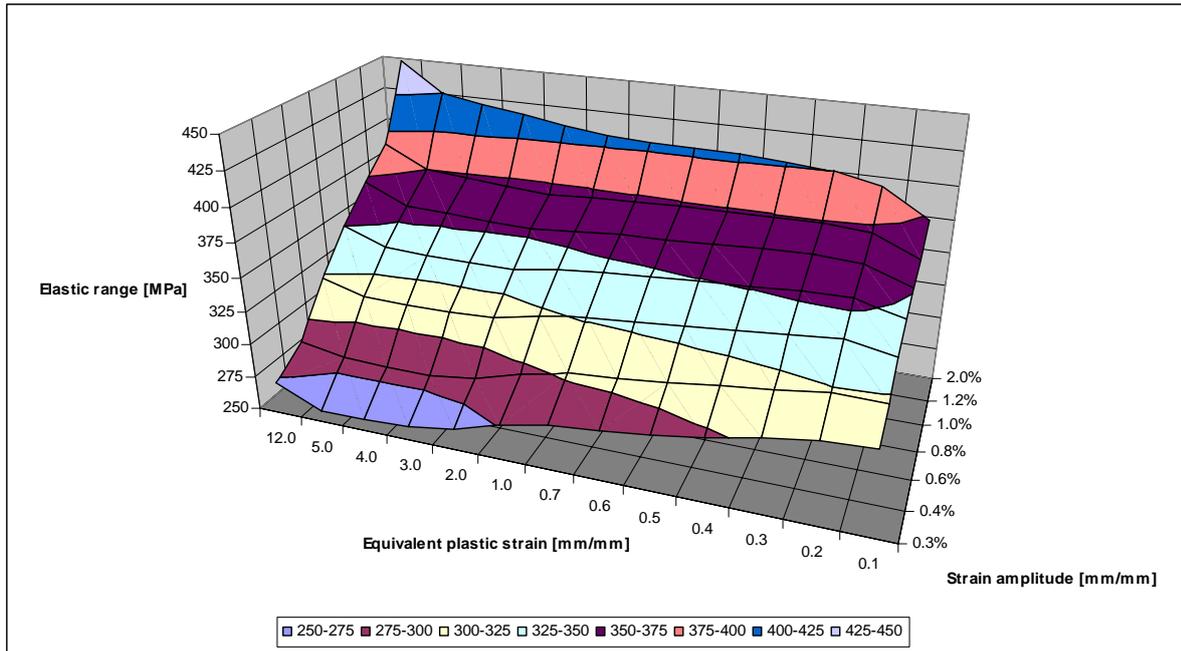12.0.

Figure 7.6   Elastic range surface according to Equation (7.2). Note arbitrary scales.
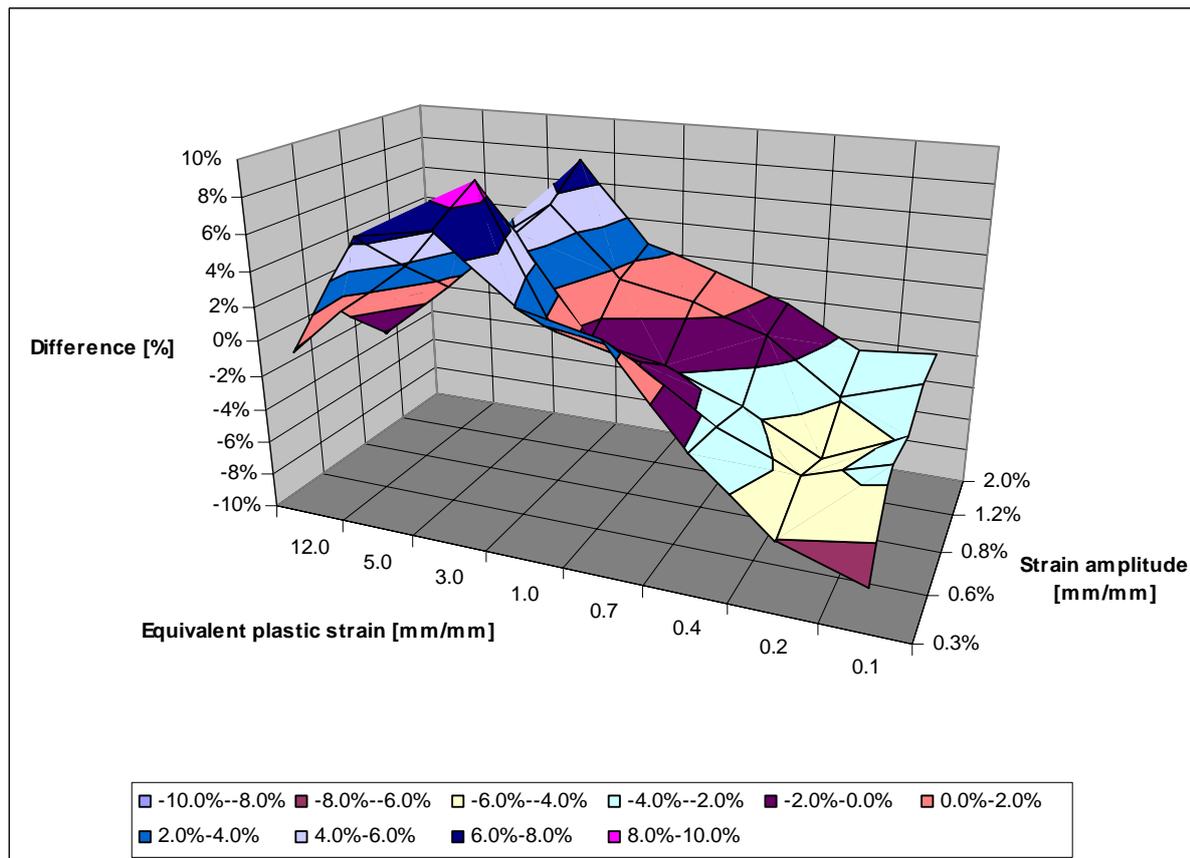

Figure 7.7   Difference between elastic ranges processed from test data and calculated according to Equation (7.2). Note arbitrary scales.

8 Conclusions

During the project an analysis tool was developed for the purpose of analysing test data of a certain test facility in order to assess the total lifetime of test specimen. Input data for FEM code ABAQUS is obtained to describe both kinematic and isotropic hardening properties. Further, by combining the result data for various strain amplitudes a mathematic expression can be created which allows defining a parameter surface for cyclic (*i.e.* isotropic) hardening. Input data for any strain amplitude within the range of minimum and maximum strain amplitudes of the test data can be assessed with the help of the developed 3D stress-strain surface presentation.

Test runs with a quadratic Timoshenko type beam element showed that ABAQUS is able to model the uniaxial stress-strain behaviour of the test specimen, as the strain amplitude is known and relevant properties for cyclic hardening can be selected. While pre-defined commands in ABAQUS let the user define only one curve for cyclic hardening properties, in engineering cases one should judge which property to choose, *i.e.* assess the maximum expected strain amplitude and select the curve accordingly. On the other hand, for FEA cases where uneven strain distributions exist, cyclic hardening property according to the highest strain amplitude causes erratic hardening at locations with lower strain amplitudes. Therefore the usability of the results of the project is limited, and more complex possibilities to define plastic material properties in ABAQUS (e.g. user-defined functions) have to be examined in forthcoming studies. Preliminary studies also indicated that simulation of variable strain amplitude loading cases requires other cyclic hardening properties than those needed in the constant strain amplitude loading cases.

All in all, one level of knowledge concerning the art of transferring test data into FEA was reached during the SAFIR research project. Apparently the next levels are 1) to define more sophisticated ways to enter plastic properties in ABAQUS and 2) to study plastic properties of variable strain amplitude loading cases.

References

1. European Commission. Nuclear Safety and Environment. Safe Management of NPP Ageing in the European Union, Final Report, 2001. 363 p.

2. Suresh, S. Fatigue of materials. Cambridge University Press, England, 1991. 586 p.

3. Sanzo, D. et al. Survey and Evaluation of Aging Risk Assessment Methods and Applications, NUREG/CR-6157. U.S. Nuclear Regulatory Commission, Washington D.C., 1994. 159 p.

4. HSE Health & Safety Executive. Best practice for risk based inspection as a part of plant integrity management. Prepared by TWI and Royal & SunAlliance Engineering for the Health and Safety Executive. CONTRACT RESEARCH REPORT 363/2001. 122+57 p.

5. Gosselin, S. (Project Manager). Risk-informed inservice inspection evaluation procedure. Electric Power Research Institute, Interim Report EPRI TR-106706. California, 1996.

6. Viswanathan, R. Damage Mechanisms and Life Assessment of High-Temperature Components. ASM International, 3rd Printing, U.S.A., 1995. 497 p.

7. Lubliner, J. Plasticity Theory. New York 1990, Macmillan Publishing Company. 495 p.

8. ABAQUS Theory manual, Version 6.3. ABAQUS Inc., 2002. Pawtucket, Rhode Island, U.S.A.

9. Lubarda, V. Elastoplasticity Theory. CRC Press. U.S., 2002.

10. Drucker, D. J. of Appl. Mech. 26, 101. 1959.

11. Hill, R. The Mathematical Theory of Plasticity, Oxford University Press. London, 1950.

12. Melan, E. Ing.-Arch. 9, 116. 1938.

13. Prager, W. Proc. Instn. Mech. Engrs. 169, 41. 1955.

14. Prager, W. J. Appl. Mech. 23, 493. 1956a.

15. Mróz, Z. J. Mech. Phys. Solids 15, 163. 1967.

16. Iwan, W. D. J. Appl. Mech. 34, 612. 1967.

17. Dafalias, Y. On Cyclic and Anisotropic Plasticity, Ph.D. thesis, Department of Civil Engineering, University of California, Berkeley. 1975.

18. Krieg, R. J. Appl. Mech. 42, 641. 1975.

19. Dafalias, Y., Popov, E. Acta Mech. 21, 173. 1975.

20. Cronvall, O., Sarajärvi, U. Treatment and numerical simulation of fatigue data of austenitic stainless piping steel. Technical Research Centre of Finland (VTT), Research Group Structural Integrity, Research Report BTUO72-041317. Finland, 2005. 47 p.

21. Cronvall, O., Sarajärvi, U. Simulation and Analysis of Data for Enhancing Low Cycle Fatigue Test Procedures. Technical Research Centre of Finland (VTT), Research Group Structural Integrity, Research Report TUO72-056604. Finland, 2006. 33 p.

22. Cronvall, O. Numerical modelling of low-cycle fatigue behaviour of austenitic stainless piping steel. Technical Research Centre of Finland (VTT), Research Group Structural Integrity, Research Report BTUO72-031200. Finland, 2004. 42 p.

23. Lemaitre, J., and J.-L. Chaboche, Mechanics of Solid Materials, Cambridge University Press, 1990.

24. Chopra, O. K. Effects of LWR coolant environments on fatigue design curves of austenitic stainless steels, NUREG/CR–5704, ANL–98/31 for U.S. Nuclear Regulatory Commission, Washington DC. USA, 1999. 42 pages.

Title	A Procedure to Generate Input Data of Cyclic Softening and Hardening for FEM Analysis from Constant Strain Amplitude Fatigue Tests in LCF Regime
Author(s)	Urpo Sarajärvi and Otso Cronvall
Affiliation(s)	VTT, Finland
ISBN	978-87-7893-213-6 *Electronic report*
Date	March 2007
Project	NKS_R_2005_40 / Corrision Fatigue
No. of pages	31
No. of tables	1
No. of illustrations	18
No. of references	24

Abstract	Fatigue is produced by cyclic application of stresses by mechanical or thermal loading. The metal subjected to fluctuating stress will fail at stresses much lower than those required to cause fracture in a single application of load. The key parameters are the range of stress variation and the number of its occurrences.
	Low-cycle fatigue, usually induced by mechanical and thermal loads, is distinguished from high-cycle fatigue, mainly associated with vibration or high number of small thermal fluctuations.
	Numerical models describing fatigue behaviour of austenitic stainless piping steels under cyclic loading and their applicability for modelling of low-cycle-fatigue are discussed in this report.
	In order to describe the cyclic behaviour of the material for analysis with finite element method (FEM) based analysis code ABAQUS, the test data, i.e. stress-strain curves, have to be processed. A code to process the data all through the test duration was developed within this study. A description of this code is given also in this report. Input data for ABAQUS was obtained to describe both kinematic and isotropic hardening properties. Further, by combining the result data for various strain amplitudes a mathematic expression was be created which allows defining a parameter surface for cyclic (i.e. isotropic) hardening. Input data for any strain amplitude within the range of minimum and maximum strain amplitudes of the test data can be assessed with the help of the developed 3D stress-strain surface presentation.
	The modelling of the fatigue induced initiation and growth of cracks was not considered in this study. On the other hand, a considerable part of the fatigue life of nuclear power plant (NPP) piping components is spent in the phase preceding the initiation and growth of cracks.
Key words	Fatigue, low-cycle, austenitic stainless steel, work hardening, modelling, FEM, ABAQUS